HHS Public Access

Author manuscript

Hippocampus. Author manuscript; available in PMC 2017 June 01.

Published in final edited form as:

Hippocampus. 2016 December ; 26(12): 1618–1632. doi:10.1002/hipo.22661.

MRI Uncovers Disrupted Hippocampal Microstructure That Underlies Memory Impairments After Early-life Adversity

Jenny Molet[1,*], **Pamela M. Maras**[2], **Eli Kinney-Lang**[2,3], **Neil G. Harris**[4], **Faisal Rashid**[3], **Autumn S. Ivy**[1], **Ana Solodkin**[1,5], **Andre Obenaus**[3], and **Tallie Z. Baram**[1,2,5]

[1]Department of Anatomy and Neurobiology, UC-Irvine, Irvine, CA, 92697-4475, USA

[2]Department of Pediatrics, UC-Irvine, Irvine, CA, 92697-4475, USA

[3]Department of Pediatrics, Loma Linda University School of Medicine, Loma Linda, CA, 92350, USA

[4]Department of Neurosurgery, UCLA, Los Angeles, CA, 90095-6901, USA

[5]Department of Neurology, UC-Irvine, Irvine, CA, 92697-4475, USA

Abstract

Memory and related cognitive functions are progressively impaired in a subgroup of individuals experiencing childhood adversity and stress. However, it is not possible to identify vulnerable individuals early, a crucial step for intervention. In this study, high-resolution magnetic resonance imaging (MRI) and intra-hippocampal diffusion tensor imaging (DTI) were employed to examine for structural signatures of cognitive adolescent vulnerabilities in a rodent model of early-life adversity. These methods were complemented by neuroanatomical and functional assessments of hippocampal network integrity during adolescence, adulthood and middle-age. The high-resolution MRI identified selective loss of dorsal hippocampal volume, and intra-hippocampal DTI uncovered disruption of dendritic structure, consistent with disrupted local connectivity, already during late adolescence in adversity-experiencing rats. Memory deteriorated over time, and stunting of hippocampal dendritic trees was apparent on neuroanatomical analyses. Thus, disrupted hippocampal neuronal structure and connectivity, associated with cognitive impairments, are detectable via non-invasive imaging modalities in rats experiencing early-life adversity. These high-resolution imaging approaches may constitute promising tools for prediction and assessment of at-risk individuals in the clinic.

Keywords

early-life stress; cognitive vulnerabilities; brain networks; magnetic resonance imaging (MRI); diffusion tensor imaging (DTI)

[*]Correspondence to: Jenny Molet, PhD, Departments of Anatomy and Neurobiology, University of California-Irvine, Med. Sci. I, ZOT 4475, Irvine, CA 92697-4475. jenny.molet@gmail.com.

INTRODUCTION

Progressive cognitive deficits including serious and worsening impairments of memory have been observed in studies of populations exposed to early-life adversity (Kaplan *et al.*, 2001; Everson-Rose *et al.*, 2003; Wilson *et al.*, 2005). Such cognitive impairments also constitute an important and relatively understudied aspect of neuropsychiatric disorders including depression and schizophrenia (Dere *et al.*, 2010; Millan *et al.*, 2012). These disorders, believed to arise from interactions between genetic and environmental influences, are especially prevalent after early-life stress and adversity (McEwen, 2003; Krishnan and Nestler, 2008; Baram *et al.*, 2012). However, cognitive problems do not affect all survivors of early-life adversity or stress, and it is not possible to predict who will be impaired. The inability to recognize individuals with incipient or emerging memory problems hampers potential targeted interventions.

Neuroimaging has been employed to assess the consequences of stress in humans (O'Doherty *et al.*, 2015) and rodent models (Bourgin *et al.*, 2015). Available neuroimaging modalities include high-resolution volumetric acquisitions, diffusion tensor imaging (DTI) and functional magnetic resonance imaging. These aim to identify structural and functional alterations resulting from chronic stress or other adversity, in the hopes of delineating biomarkers of cognitive or emotional deficits. The goal of the current study was two-fold. First, we wished to examine for functional deficits in hippocampal function after early life adversity. Second, we undertook non-invasive magnetic resonance imaging (MRI) to determine if the observed functional hippocampal problems could be visualized by imaging, as might be done clinically. Here, using a well-characterized rodent model of early-life adversity, we demonstrate progressive deficits in both object memory and in hippocampus-dependent spatial memory. We then employ high-resolution MRI and intra-hippocampal diffusion tensor imaging (DTI) combined with regional analysis to provide a unique systems view of the hippocampus, to probe the structure and connectivity of the hippocampus. We find selective loss of dorsal hippocampal volume and disrupted dendritic microstructural organization already during late adolescence, when nascent memory problems emerge. We then identify the neuro-anatomical basis of these novel MRI changes. Together, these studies indicate that disrupted hippocampal neuronal structure and connectivity are detectable early using non-invasive imaging modalities, with broad clinical implications.

MATERIALS AND METHODS

Experiments were performed in accordance with NIH guidelines and approved by the Institutional Animal Care and Use Committee.

Animals and Experimental Paradigms

Subjects were born to timed-pregnant Sprague-Dawley rat dams maintained in uncrowded animal facilities on 12 h light/dark cycles with access to chow and water. On P2, pups from several litters were gathered, and 12 (6 males; 6 females) were assigned at random to each dam, to obviate potential genetic and litter size confounders. After weaning, males were housed two to three per cage.

The Early-Life Stress/Adversity Paradigm (CES)

The early-life stress/adversity paradigm (CES) consisted of limiting nesting and bedding materials in cages between P2–P9 (Brunson *et al.*, 2005; Molet *et al.*, 2014). For the CES group, cages were fitted with a plastic-coated aluminum mesh platform ~2.5cm above the floor (allowing for collection of droppings). Bedding was reduced to cover cage floor sparsely, and one-half of a single paper towel was provided for nesting material. Control (CTL) dams and litters resided in standard cages containing 0.33 cubic feet of cob bedding. In this paradigm, maternal care was fragmented and unpredictable, provoking chronic stress in the pups (Ivy *et al.*, 2008; Molet *et al.*, 2014; Molet *et al.*, 2016). Control and experimental cages were undisturbed during P2–P9, housed in temperature-controlled rooms with laminar airflow preventing ammonia accumulation. On P10, experimental groups were transferred to routine cages, where maternal behavior normalized within hours (Ivy *et al.*, 2008; Molet *et al.*, 2014). Rats were weaned on P21–22, and then housed in group cages.

Adolescent Short Stress

CTL and CES rats (7–8 weeks) were exposed to 5h concurrent physical, psychological and social stresses (Maras *et al.*, 2014). Briefly, rats were restrained and crowded six to a cage, which was placed on a laboratory shaker in a brightly lit room bathed in loud rap music (90 dB) for 5 h. Rats were returned to home cages for 24 h, then trained and tested for memory.

Memory Tests

Rats were tested for object recognition (OR) (n =6–11/group) (Maras, Molet et al., 2014) or in the more stringent and more hippocampus-dependent object location task (OL) (n =17–21/group) (Squire *et al.*, 2007; Broadbent *et al.*, 2010; Langston and Wood, 2010). These consisted of two phases conducted over 2 days: a training session (24 h after termination of the adolescent short stress, or “second hit”) and a testing phase (24 h after training). Rats from each of the experimental groups (CTL, CTL+, CES, CES+) were run concurrently and at the same time of day.

During the training session on day 1, rats were placed in the experimental apparatus with two identical objects (A1 and A2). These included a yellow radioactivity container or a clip for the object recognition test, and 250-mL beakers for the object location. Rats were allowed to explore the objects for 10 min. In the OR test, the objects for training were counterbalanced across groups and all objects were cleaned with 70% ethanol between trials. During the testing session on day 2, rats were returned to the testing room, placed in the experimental apparatus and allowed to explore the two objects for 5 min. In the OR task, animals were presented with a familiar object from the training session and a novel object (either yellow radioactivity container or clip). In the OL task, rats were presented with the two familiar objects from the training session with one object moved to a novel location. Both training and testing phases were video-recorded using an overhead camera, and the duration of exploration of each object (touching the object with the nose or sniffing with the nose <2 cm from objects) as well as total object exploration were scored without the knowledge of group. To assess recognition memory of the familiar object, exploration times (t) for the novel (N) and familiar (F) objects were used to calculate a discrimination ratio (Novel/Familiar) and a discrimination index (DI) for each subject, which reflects the

preferential exploration of the novel object while taking into account any differences in total object exploration: DI =(tN − tF)/(tN +tF).

Magnetic Resonance Imaging (MRI)

We used ultrahigh-resolution MRI scanners (11.7T for neuroanatomy, 9.4T for DTI), and long acquisition times. To avoid motion artefacts, we imaged brains post-mortem. Two cohorts of CTL and CES rats (n =9/group) were sacrificed via transcardiac perfusion using 4% paraformaldehyde (PFA). Whereas imaging of either the brain in the cranial vault (Papp *et al.*, 2014) or of the brain alone have been reported, brain-only samples have been used to generate atlases (Kovacevic *et al.*, 2005). Therefore, we elected to remove the brains from the cranial vault. Brains were postfixed in 4% PFA, washed and stored at 4°C in 0.1M PB/0.05% azide. Together, these procedures reduced the potential for artifacts particularly at high field strengths. Prior to imaging, brains were placed in Fluorinert to facilitate susceptibility matched imaging.

On a Bruker Avance scanner (Bruker Biospin, Billerica, MA), we employed 3D Rapid Acquisition with Relaxation Enhancement (3DRARE), with a 256^3 matrix, 2 cm field of view and 78-μm slice thickness, repetition time/echo =2,388/15 ms and a single average. The 5 h imaging yielded 78 × 78 × 78 μm/pixel isotropic resolution. High-resolution DTI-MR images were acquired using a 9.4T Bruker Biospin MRI system (Paravision 5.1). Brains were positioned in 5-ml plastic syringes and submerged in Fluorinert. Each acquisition consisted of 50 0.5 mm slices, 1.922 cm field of view, 128 × 128 matrix zero-filled to 256 × 256 at reconstruction. Four-shot echo-planar imaging was used to acquire four averages of diffusion weighted images with b =0 (5 images) and b =3,000 s mm^{-2} (30 images in noncolinear directions); diffusion pulse width =4 ms; interpulse =20 ms; repetition time =12,500 ms; echo time =36 ms. The resultant DTI scans yielded an acquired in-plane resolution of 150 μm and a reconstructed resolution of 75 μm. The 0.5-mm slice thickness was utilized to optimize signal to noise whilst minimizing total scan time (1 h 56 min).

We avoided the use of exogenous contrast agents for several reasons: (1) the anatomical boundaries of the rodent hippocampus are readily discernible on standard neuroimaging protocols, so the potential improvements in visualization of brain anatomy, particularly when ex vivo imaging is employed (Norris *et al.*, 2013), was less important here; (2) ultimately, we wished to use a neuroimaging protocol that is clinically translatable and use of contrast agents typically are not considered routine for structural imaging.

Volumetric Analysis

Brains were realigned along a horizontal axis from anterior commissure to posterior commissure using ImageJ, so that ventral hippocampus was present >200 μm in the coronal plane before appearance of most anterior dorsal hippocampus. Volumetric analyses of total brain, ventricles and hippocampi were performed on coronal slices using Cheshire image processing (Hayden, Waltham, MA) by investigators unaware of treatment groups. Regions of interest were manually delineated and separate analyses undertaken of left and right brain along the entire rostrocaudal extent of hippocampus, using anatomical landmarks. Using external landmarks avoided potential confounders of treatment-specific changes in

hippocampal shape or volume. Mid-dorsal hippocampus was defined here as consisting of the four anterior-most slices (1248 μm) where all hippocampal subregions were visible. Within these landmark-driven boundaries, hippocampus, ventricles and hemispheres were delineated in every fourth slice (312 μm interslice distance). To calculate volumes, interpolated areas were computed from the actual areas using cubic spline function (MATLAB MathWorks, Natick, MA); volumes of brain, left and right total hippocampus, left and right mid-dorsal hippocampus, and left and right ventral hippocampus were calculated by summing the interpolated 2D areas × slice thickness (78 μm).

We performed manual (rather than automated) segmentation here for the following reasons. (A) Direct comparisons between manual and automated segmentation have reported that subtle volumetric alterations may not be detected when imaging data are morphed to a standardized atlas (Hayes et al., 2014). Similarly, over-estimation of hippocampal volumes was found upon use of two separate automated segmentation methods (Schoemaker et al., 2016). (B) As noted in the results, we found that only moderate dendritic changes, so that it is likely that morphing to template atlases might have obliterated small, yet biologically important differences. (C) We found a significant increase in ventricular volumes that was commensurate with hippocampal volume loss. This was associated with altered ventricular shape, which might render morphing of data to atlases more problematic. (D) Whereas it is quite likely that proprietary or institution-generated atlases exist, there are few (if any) widely available atlases that are based on tensor or voxel based morphometry for rats. Together, these considerations led us to manual segmentation approaches as equal to, and perhaps superior to, automated algorithms for the purpose of this study.

Diffusion Tensor Analyses

Initial analysis was performed using DSI Studio (National Taiwan University). Fractional anisotropy and primary, secondary, and tertiary diffusion eigenvector maps were calculated using FSL. Regions of interest (ROI) were drawn over the right and left CA1 dendritic region (stratum radiatum, SR) of two adjacent slices encompassing dorsal hippocampus, guided by atlases for each animal (Fig. 3A). CA1 SR region was manually delineated using the primary eigenvector map color-coded for direction and modulated by FA, which provided superior delineation for each pixel. CA1 SR was defined as commencing two pixels below corpus callosum to exclude stratum pyramidal and 14–20 pixels long based on FA values. The ROIs from each animal were then placed onto their respective eigenvalue, radial diffusivity and FA maps, and values were derived using FSL tools.

Radioimmunoassay

Plasma corticosterone levels were measured together at 0, 60, 90 min and 5 h from onset of 5 h stress in two cohorts (n =12/group), using a kit (MP Biomedicals, Solon, OH) as described (Rice *et al.*, 2008). Assay sensitivity was 0.5 μg dL^{-1} and all samples were run in a single assay.

Golgi-Cox Impregnation and Quantification of CA1 and CA3 Pyramidal Cell Dendrites

Eight-week old CES and CTL rats (n =3–4/group) were euthanized and perfused with 0.9% saline, pH7.4 Brains were removed into Golgi–Cox solution and coronal slices from the

hippocampus (200 μm) were cut. Fully impregnated CA1 and CA3 neurons were imaged and reconstructed without knowledge of treatment group (n =6–10 neurons/rat). Dendritic arborization was analyzed using Sholl's method (Sholl, 1953) which provides a quantitative description of the dendritic tree by counting the number of dendrites that cross virtual concentric circles drawn at fixed distance from the soma.

Statistical Analyses

All measurements and analyses were performed without knowledge of group. Two-way analysis of variance (ANOVA) was used for discrimination ratio, discrimination index values and total exploration times. Two-way repeated-measures (RM)-ANOVA was used for analyses the time course effect of the early-life stress in OR, corticosterone levels and Sholl analyses of dendrites. Early-life treatment group was used as the "between-subjects" factor, and age (OR), time elapsed from the start of stress (corticosterone) or distance away from soma (Sholl) was used for the "within-subjects" factor. Two-way ANOVAs were followed by Bonferroni's post hoc multiple comparisons test. Student's t tests (two-tailed unpaired) were used to compare total apical dendritic length and hippocampal, brain and ventricle volumes across early-life treatment group. All MR data (volumetric and DTI) were assessed using one way ANOVA for group and left/right differences followed by Tukey post-hoc analysis. Outliers were assessed using interquartile ranges and removed from final analysis. Significance levels were set at 0.05, and data are presented as mean ±SEM. Statistical analyses were performed using GraphPad Prism 5.0 software (GraphPad, San Diego, CA).

RESULTS

Early-Life Adversity Leads to Progressive Memory Deficits

Rats reared in conditions promoting chronic early-life stress (CES) (Brunson *et al.*, 2005; Molet *et al.*, 2014) performed well in the object recognition (OR) test at 4 and 8 months of age (Fig. 1A). Specifically, the discrimination index (DI) a measure of novel object preference, was similar in rats reared under typical laboratory conditions (CTL) and the CES group (DI: 0.27 ±0.07 *vs.* 0.28 ±0.1 at 4 months; 0.29 ±0.04 *vs.* 0.23 ±0.07 at 8 months). Using ratios of time exploring novel *vs.* familiar object as a measure of memory yielded the same results: (1.87 ±0.28 *vs.* 2.06 ±0.48 at 4 months; 1.89 ±0.18 *vs.* 1.69 ±0.22 at 8 months, *post hoc* P >0.05, Table 1). However, by 12 months, object memory declined in CES rats (Brunson *et al.*, 2005; Ivy *et al.*, 2010) (DI: −0.03 ±0.03 *vs.* 0.37 ±0.04; ratio: 0.94 ±0.06 *vs.* 2.57 ±0.20; all P <0.01, Fig. 1). Two-way RM-ANOVA revealed effects of CES ($F_{1,10}$ = 7.96; P =0.02) and interaction of CES and age ($F_{2,20}$ = 6.80; P <0.01). Whereas total exploration times decreased with age (training: $F_{2,20}$ = 30.34; P <0.01; testing: $F_{2,20}$ = 15.29; P <0.01), they did not differ among groups (all P >0.05, Table 1).

Vulnerabilities of Memory Function Emerge Already during Late Adolescence

The findings described above were consistent with several possible scenarios. Either the CES led to no immediate consequence yet unleashed a delayed toxic effect on hippocampal function with onset in middle-age. Alternatively, CES initiated an effect that remained latent up to middle-age, and hence might be unmasked by appropriate provocation ("second hit"). To probe the latter possibility, we tested 7- to 8-week old (late-adolescent) rats for their

ability to remember an object following an acute challenge. Both CTL and CES adolescent rats spent more time exploring the novel object and their discrimination indices and ratios did not differ appreciably (DI: 0.39 ±0.04 *vs.* 0.38 ±0.04; Fig. 1B; ratio: 2.42 ±0.25 *vs.* 2.41 ±0.26 all $P>0.05$, Table 2). We then examined if the object memory of CES rats, dependent on intact limbic circuitry (Squire *et al.*, 2007) might be compromised by challenges. We exposed subgroups of both CTL and CES rats to a 5 h combined stress and tested them after a 24 h recovery. Exploration times for the objects were comparable in the challenged (CTL +; CES+) and nonchallenged groups during both training and testing (Table 2). However, whereas performance in the memory task was not influenced by stress experienced 24h earlier in CTL rats (DI: 0.40 ±0.03 *vs.* 0.39 ±0.04, Fig. 1B; ratio: 2.42 ±0.19 *vs.* 2.42 ±0.25, Table 2; all $P>0.05$), the performance of challenged CES rats was drastically impaired, with novel/familiar ratio =1.44 ±0.20 in CES+; 2.41 ±0.26 in CES. DI was significantly lower in CES+ rats compared with CTL+ (0.13 ±0.06 *vs.* 0.38 ±0.04, Fig. 1B). These results indicated that rats experiencing CES were cognitively vulnerable: a “second hit” unmasked incipient memory deficits that were not apparent when the test was performed under routine circumstances.

Hormonal Responses to a Second Stress Are Not Altered in Adolescent Rats Reared Under Adversity

The adverse effects of stress on memory in CES rats might derive from enduringly heightened sensitivity to stress: stress might elicit a more robust or protracted neuroendocrine response from these rats, differentially affecting their performance 24 h later. To test this possibility, we measured the time-course of plasma corticosterone in separate groups of CTL+ and CES+ rats exposed to identical 5 h stress (Fig. 1C). Basal corticosterone levels did not differ between groups (two-way RM-ANOVA, early-life experience effect: $F_{1,22} = 0.52$; $P>0.05$). In addition, neither plasma corticosterone at 60min from stress onset nor the decay slope distinguished CTL+ from CES+ rats (early-life experience x time interaction: $F_{3,66} = 1.15$; $P>0.05$). Thus, differential sensitivity to stress in CES rats did not explain the cognitive vulnerability of this group.

Early-life Adversity Provokes Overt Memory Deficits in an Hippocampus-dependent Spatial Memory Test

If rats experiencing CES perform poorly in the OR test when challenged but not under basal conditions, then it is likely that this vulnerability might be unmasked by more rigorous or more hippocampus-selective memory tests, revealing overt memory deficits. Accordingly, the ability to remember the location/placement of objects (OL), a spatial memory test requiring an intact mid-dorsal hippocampus (McQuown *et al.*, 2011; Vogel-Ciernia and Wood, 2014), was impaired in late adolescent CES rats even without exposure to a 2nd challenge (two-way ANOVA, early-life stress effects: $F_{1,73} = 15.49$; $P<0.01$; Fig. 1D). Specifically, CTL and challenged-CTL (CTL+) rats performed well in the OL task, apparent from their DI and new/old location ratios (DI: CTL =0.30 ±0.04; CTL+=0.25 ±0.05 Fig. 1D; ratio: CTL =2.10 ±0.25; CTL+=1.9 ±0.19, Table 3). However, CES rats did significantly worse than CTL both before and after challenge (DI: CES =0.08 ±0.06, CES+=0.02 ±0.04 Fig. 1D, ratio: CES =1.36 ±0.18, CES+=1.10 ±0.09; all $P<0.01$). Notably, exploration times of all groups during both training and testing, as well as other parameters of the test, did not

distinguish among groups (Table 3). Together, these results indicated that CES provoked hippocampal functional deficits already during late adolescence. These deficits were not sufficient to impair performance in OR. However, they became evident with the use of either an adolescent stress challenge or upon more rigorous tests that require intact dorsal hippocampus (Maras *et al.*, 2014; Vogel-Ciernia and Wood, 2014).

High-resolution Magnetic Resonance Imaging Detects Selective Loss of Dorsal Hippocampus Volume Loss after Early Life Adversity

The spatial memory deficits observed in CES rats already at 7–8 weeks suggested that the hippocampal network responsible for memory was impaired, raising the possibility that CES interfered with normal hippocampal growth and maturation patterns. If such structural consequences of early-life adversity existed and are detectable using non-invasive methods in rodents, they might be instructive about the human condition. Indeed, several studies have described reductions in hippocampal volumes using MRI following childhood trauma and adversity (Bremner *et al.*, 1997; Bremner *et al.*, 2003; Woon and Hedges, 2008). In human studies, it is difficult to infer causality and it is not known if an observed volume reduction results from CES, or from genetic (Lyons *et al.*, 2001; van Haren *et al.*, 2004) or other unidentified factors. Therefore, we employed high-resolution anatomic MRI to probe hippocampal volume and DTI to assess hippocampal microstructure. We focused on the mid-dorsal hippocampus because it is crucial for spatial memory (McQuown *et al.*, 2011).

High-resolution visualization of internal hippocampal structure and layers and matching of sections within dorsal hippocampus among individual brains from both groups were enabled by 3D-RARE acquisitions; these yielded virtual sections 78 μm in thickness (Fig. 2A). Comparing volumes of mid-dorsal hippocampus between groups (n =9/group), we found significantly reduced volume of the left side in CES (4.84 ±0.12 mm^3) vs. CTL rats (5.26 ±0.15 mm^3; t_{16} = 2.19, P =0.04; Fig. 2B,C). The volume loss in CES hippocampi was limited to a relatively confined region of mid-dorsal hippocampus which, in itself, accounted for ~10% of total hippocampal volume (total volume of left hippocampus: 42.58 ±0.44 mm^3 and 42.58 ±0.48 mm^3 in control and CES groups, respectively). Therefore, as expected, the reduction in volume of this small hippocampal subregion did not impact total hippocampal volume significantly (Fig. 2D) and was associated only with a trend towards a modest increase in the left ventral hippocampus volume (35.52 ±1.4 mm^3 and 35.78 ± 1.5 mm^3 in control and CES, respectively). Whole brain volumes also did not distinguish between groups (Fig. 2E). The selective reduction of mid-dorsal hippocampal volume was associated with a commensurate increase of the volume of the dorsal portions of the lateral ventricles in the CES group, measured on the same anatomical sections (CES: 5.17 ±0.40 mm^3, CTL: 4.19 ±0.23 mm^3, t_{16} = 2.12, P =0.05, Fig. 2B).

Diffusion Tensor Imaging Detects Adversity-provoked Disruption of Hippocampal Dendritic Architecture

The observed loss of dorsal hippocampal volume might be a result of a reduction of one or several of its components. Structurally, the hippocampus (and therefore its volume) is comprised of dendrites, glia, extracellular matrix and neuronal cell bodies and axons (Paus, 2009), and the dendritic trees account for ~30% of the total volume. Therefore, we examined

here the possibility that diminished dendritic arborization, described in middle-aged rats after early-life adversity (Brunson *et al.*, 2005; Ivy *et al.*, 2010), contributed to the dorsal-hippocampus volume loss. We capitalized on hippocampal organization: Within area CA1, apical dendritic trees are oriented perpendicular to the pyramidal cell layer, providing a highly organized structure (Fig. 3A,B). We conducted intra-hippocampal DTI, a method that reports on directional water diffusion and that has been used to detect microstructural alterations in pathological conditions in humans and experimental models (Ayling *et al.*, 2012; Shenton *et al.*, 2012). Multiple metrics can be derived from DTI including individual directional eigenvalues (λ1, λ2, λ3), axial (AD) and radial (RD) diffusivities and fractional anisotropy (FA). Using DTI we queried if CES provoked DTI-detectable hippocampal disorganization. In addition, because of the laterality of hippocampal volume changes in CES hippocampus, we assessed the left and right sides separately.

Fractional anisotropy (FA; a measure of the anisotropy of water diffusion) was increased in dendritic layers of left hippocampal CA1 (Fig. 3B,C) of 2-month-old CES rats ($P<0.01$) but not on the right ($P=0.2$) (Fig. 3C and Table 4). The increased FA implies that the water diffusion was more anisotropic in CES dendritic layers, a factor governed by dendritic microstructure (Fig. 3D). The increased FA resulted from combined trends for changes in water mobility along the plane of the main apical dendritic stem (λ1) and within the plane of the commissural-associational and Schaeffer collateral branching (λ2), without discernible differences in the anterior-posterior direction (λ3) or radial diffusivity (RD =(λ2+λ3)/2) (Fig. 3E and Table 4). These findings were confined to the left hippocampus, in line with the volume changes, and suggested loss of integrity of hippocampal apical dendritic trees, prompting us to examine these directly.

The Structural Neuroanatomical Correlates of Imaging-detected Hippocampal Deficits in Rats Experiencing Early-life Adversity

Because dendritic trees contribute significantly to both hippocampal volume and microstructure and their integrity is crucial for normal memory, we examined the structure of apical dendritic trees of CA1 and CA3 pyramidal cells in dorsal hippocampus of CES vs. control rats.

Total apical dendritic length in CA1 and CA3 neurons was diminished in 8-week-old CES rats compared to CTL (1376 ± 81.48 vs. 1655 ±81.70 μm, $t_{17} = 2.42$, $P=0.03$; 1655 ±90.66 vs. 2053 ±137.3 μm, $t_{19} = 2.52$, $P=0.02$; respectively; Fig. 4A,B). This reduction seemed to derive from loss of dendritic branches mainly in the proximal tree, site of innervation of commissural/associational fibers and Schaefer collaterals, key pathways for information flow within hippocampus (arrows Fig. 4A). The complexity of dendritic arborization was reduced in both CA3 and CA1. In CA3 a significant early-life stress effect ($F_{22,110} = 2.99$; $P<0.01$), a distance from soma effect ($F_{22,110} = 50.22$; $P<0.01$) and an early-life stress x distance from soma interaction were noted ($F_{1,5} = 13.24$; $P=0.02$; Fig. 4D). In area CA1, an interaction of early-life stress x distance from soma was observed ($F_{17,85} = 3.49$; $P<0.01$), as well as a distance from soma effect (two-way RM-ANOVA, $F_{17,85} = 45.12$; $P<0.01$; Fig. 4C). These findings indicate that dorsal hippocampus structure is impacted by CES already

during late adolescence, and the process was more advanced in area CA3, as reported at older ages (Brunson *et al.*, 2005; Ivy *et al.*, 2010).

DISCUSSION

The principal findings of the present studies are: (a) Cognitive vulnerabilities exist in late adolescent rodents that had experienced early-life adversity and progress to overt pathology with age. (b) These vulnerabilities can be unmasked by a “second hit” consisting of a short stress, or by the use of more rigorous and hippocampus-dependent tests. (c) Clinically relevant imaging methods, including high-resolution, intra-hippocampal DTI, can visualize hippocampal volume loss and microstructural deficits and may allow diagnosis of cognitive vulnerabilities in humans.

Early-life adversity is strongly associated with neuropsychiatric disorders such as depression and schizophrenia, in which significant and progressive memory deficits accompany emotional impairments (Millan *et al.*, 2012). Additionally, early-life adversities such as rearing in orphanages or maltreatment are associated with reduced cortical and hippocampal volumes (Teicher *et al.*, 2012; Hodel *et al.*, 2015). Whereas causality for both outcomes is difficult to infer in human populations where numerous factors might interact, we probed causality in rodents by artificially imposing adversity during a defined developmental period. We reared rats in early-life adversity environment during P2–P9 which, for hippocampal development, represents late gestation and early infancy periods (Avishai-Eliner *et al.*, 2002), then normalized the environment. We found seemingly normal memory using a typical object recognition test (Broadbent *et al.*, 2010). However, memory disintegrated in CES rats when tested 24 h after a short stress, and deficits progressed in all CES rats, associated with abnormal hippocampal volume and structure on MRI.

How might early-life adversity/stress impact hippocampal microstructure and volume? CES may both interfere with the normal construction and maturation of cortical and hippocampal networks, as well as promote their destruction (Kehoe and Bronzino, 1999; Brunson *et al.*, 2005; Radley *et al.*, 2008; Maras *et al.*, 2014). In middle-aged CES rats, impoverished dendritic trees and reduced hippocampal volume have been described (Brunson *et al.*, 2005; Ivy *et al.*, 2010), and similar dendritic changes were found in prefrontal cortex (Radley *et al.*, 2008). Because dendrites comprise ~42% of cortical volume (Paus, 2009) and dendritic impoverishment correlated with hippocampal volume loss in rodents, it is reasonable to assume that cortical and hippocampal volume reduction in human adolescents and adults exposed to early-life adversity might derive from abnormal growth and branching of neuronal dendrites.

The relationship of dendritic arborization and memory has been established and both can result from stress (Magarinos and McEwen, 1995; Brunson *et al.*, 2005; Radley *et al.*, 2008; Ivy *et al.*, 2010; Maras *et al.*, 2014). In mature brain, stress induces structural changes that depend on its duration. Modifications of the synaptic machinery take place within minutes (Chen *et al.*, 2008). Loss of spines and the excitatory synapses they carry (Bourne and Harris, 2008; Holtmaat and Svoboda, 2009) takes place within hours, and correlates strongly with memory in individual mice (Chen *et al.*, 2010). Chronic stress leads remodels dendritic

branches (Kim *et al.*, 2010; McEwen, 2012), presumably because dendritic integrity requires functional excitatory synapses on dendritic spines. Indeed, rapid, stress-induced dendritic spine loss is found in the distribution of eventual dendritic atrophy in adult hippocampus (Pawlak *et al.*, 2005; Chen *et al.*, 2008). Therefore, a potential scenario for the effects of CES on memory involves loss of synapses and spines mediated by stress hormones including corticosterone and hippocampal CRH (Chen *et al.*, 2008; Segal *et al.*, 2010). This loss both interferes with memory processes and promotes dendritic stunting/atrophy (Regev and Baram, 2014).

Notably, dendritic disruption may progress with age, as supported by studies using transgenic mice (Wang *et al.*, 2011, 2012). Mice with a conditional knock-out of the CRFR1 gene were resistant to enduring cognitive defects that follow CES. CES took place during the first postnatal week, prior to repression of CRFR1 receptor via CaM Kinase II mechanisms [the latter is expressed commencing P5–P10, with full maturation by P20; (Wang et al., 2011)]. Thus whereas CRFR1 receptors were still expressed during the first 10 days of life, the CES period, their absence later was protective, suggesting that memory deficits require progressive processes beyond the CES period. Epidemiological studies in humans also suggest a progressive injury: cognitive problems in individuals with evidence of CES emerge during middle-age and are a risk-factor for early dementia (Kaplan *et al.*, 2001). Whereas studies on children subjected to early-life emotional deprivation followed by environmental enrichment (Nelson *et al.*, 2007) support a sensitive (critical) period for the major effects of CES, cognitive impairments over the lifetime may reflect cumulative effects of both early and continuing processes (Ulrich-Lai and Herman, 2009). The evidence for progression CES effects beyond infancy thus offers an important opportunity for interventions.

Here we demonstrate the use of noninvasive imaging methods to detect disruption of hippocampal structure already during late-adolescence/early adulthood, with the development of ultra-high magnetic field strength and spatial resolution as mesoscopic MRI techniques. We visualized the impoverished dendritic trees using high-resolution MR imaging. Notably, the volume of the human brain is >1,000 cubic centimeters (cc), compared with the ~2cc volume of the adolescent/adult rat. To enable sufficient resolution, we used a high-field magnetic resonance imaging scanner (11.7 Tesla). The availability of high-resolution quantitative neuroimaging has enabled such intra-hippocampal DTI approaches in humans, albeit in a research setting (Yassa *et al.*, 2010). Kerchner et al., 2010 detected of hippocampal neuropil loss and DTI at 3.0T in human infants has been reported to be sensitive to developmental maturation of the dendritic microstructure (Trivedi *et al.*, 2009; Ball *et al.*, 2013). Together, these encouraging developments suggest that the methodologies described here might have clinical potential in the future.

This study is among the first to correlate memory deficits induced by early-life adversity with disrupted hippocampal microstructure by combining histology and DTI to assess the integrity of the organized dendritic layers within hippocampus. DTI has been extensively utilized in humans and rodents to measure water diffusion, typically in ordered white matter axonal bundles (Qiu *et al.*, 2015). There are few reports of gray-matter DTI and fewer yet in rodents (Keller *et al.*, 2012; Laitinen *et al.*, 2015). Thus, our ROI analysis of hippocampal

gray matter using DTI is relatively new. Hippocampal plasticity via manual ROI delineation has been examined in rodents (Sierra *et al.*, 2015) and in humans (Goubran *et al.*, 2015). These studies did not focus on the dendritic regions but included all hippocampal structures. In addition, previous ex vivo DTI studies that have pushed the boundaries to increase resolution have not been clinically relevant, demanding hours-long imaging times (Zhang *et al.*, 2002; Calamante *et al.*, 2012). Here, we aimed to employ *ex vivo* imaging, with its superior signal to noise ratio as an initial step towards in vivo imaging. Therefore, we used specifically imaging sequences employed routinely for in vivo imaging.

We found increased FA in hippocampal dendritic regions together with volume loss after CES. Similar associations between FA and volume were found in human Alzheimer's and mild cognitive impairments (Kantarci, 2014), as well as temporal lobe epilepsy (Kim *et al.*, 2010; Keller *et al.*, 2012). In animal models of brain trauma, decreased FA in CA1 (all cellular layers) was associated with radial diffusivity ($\lambda 2+\lambda 3/2$) whereas increased FA in CA2/3 associated with axial diffusivity ($\lambda 1$) (Sierra *et al.*, 2015). In a model of CES (Zalsman *et al.*, 2015) increased FA in dentate gyrus correlated with altered measures of depression, and a single communication described increased FA correlating with decreased dendritic densities (Pych *et al.*, 2008). Thus, hippocampal gray matter DTI in humans and in rodents may provide surrogate markers for emerging neuropathology.

Overall, our results show that cognitive vulnerabilities exist in late adolescent rodents that had experienced early-life adversity and which then progress to overt pathology with age. These vulnerabilities can be unmasked by a short challenge or by the use of more rigorous and hippocampus-dependent tests. The neuroanatomical basis of these vulnerabilities involves reduced dendritic arborization within the hippocampus. Importantly, clinically relevant imaging methods, including high-resolution intra-hippocampal DTI, allow visualization of hippocampal volume loss and microstructural deficits in the rodent after early life stress. These findings are important, because they indicate that we can detect early and non-invasively disrupted hippocampal neuronal structure and connectivity which predict memory problems. These findings allow translation to clinical populations at risk for these cognitive problems following early-life adversity.

Acknowledgments

The authors thank Mr. Tad Foniok, Mr. David Rushforth, and Dr. Jeffery Dunn (U. Calgary) for assistance in DTI, and Dr. Yuncai Chen for help with figures.

Grant numbers: MH73136, NS29012, P50MH096889.

References

Avishai-Eliner S, Brunson KL, Sandman CA, Baram TZ. Stressed-out, or in (utero)? Trends Neurosci. 2002; 25:518–524. [PubMed: 12220880]

Ayling E, Aghajani M, Fouche JP, van der Wee N. Diffusion tensor imaging in anxiety disorders. Curr Psychiatry Rep. 2012; 14:197–202. [PubMed: 22460663]

Ball G, Srinivasan L, Aljabar P, Counsell SJ, Durighel G, Hajnal JV, Rutherford MA, Edwards AD. Development of cortical microstructure in the preterm human brain. Proc Natl Acad Sci USA. 2013; 110:9541–9546. [PubMed: 23696665]

Baram TZ, Davis EP, Obenaus A, Sandman CA, Small SL, Solodkin A, Stern H. Fragmentation and unpredictability of early-life experience in mental disorders. Am J Psychiatry. 2012; 169:907–915. [PubMed: 22885631]

Bourgin J, Cachia A, Boumezbeur F, Djemai B, Bottlaender M, Duchesnay E, Meriaux S, Jay TM. Hyper-responsivity to stress in rats is associated with a large increase in amygdala volume. A 7T MRI study. Eur Neuropsychopharmacol J Eur Coll Neuropsychopharmacol. 2015; 25:828–835.

Bourne JN, Harris KM. Balancing structure and function at hippocampal dendritic spines. Annu Rev Neurosci. 2008; 31:47–67. [PubMed: 18284372]

Bremner JD, Randall P, Vermetten E, Staib L, Bronen RA, Mazure C, Capelli S, McCarthy G, Innis RB, Charney DS. Magnetic resonance imaging-based measurement of hippocampal volume in posttraumatic stress disorder related to childhood physical and sexual abuse—A preliminary report. Biol Psychiatry. 1997; 41:23–32. [PubMed: 8988792]

Bremner JD, Vythilingam M, Vermetten E, Southwick SM, McGlashan T, Nazeer A, Khan S, Vaccarino LV, Soufer R, Garg PK, Ng CK, Staib LH, Duncan JS, Charney DS. MRI and PET study of deficits in hippocampal structure and function in women with childhood sexual abuse and posttraumatic stress disorder. Am J Psychiatry. 2003; 160:924–932. [PubMed: 12727697]

Broadbent NJ, Gaskin S, Squire LR, Clark RE. Object recognition memory and the rodent hippocampus. Learn Mem. 2010; 17:5–11. [PubMed: 20028732]

Brunson KL, Kramar E, Lin B, Chen Y, Colgin LL, Yanagihara TK, Lynch G, Baram TZ. Mechanisms of late-onset cognitive decline after early-life stress. J Neurosci. 2005; 25:9328–9338. [PubMed: 16221841]

Calamante F, Tournier JD, Smith RE, Connelly A. A generalised framework for super-resolution track-weighted imaging. NeuroImage. 2012; 59:2494–2503. [PubMed: 21925280]

Chen Y, Dube CM, Rice CJ, Baram TZ. Rapid loss of dendritic spines after stress involves derangement of spine dynamics by corticotropin-releasing hormone. J Neurosci. 2008; 28:2903–2911. [PubMed: 18337421]

Chen Y, Rex CS, Rice CJ, Dube CM, Gall CM, Lynch G, Baram TZ. Correlated memory defects and hippocampal dendritic spine loss after acute stress involve corticotropin-releasing hormone signaling. Proc Natl Acad Sci USA. 2010; 107:13123–13128. [PubMed: 20615973]

Dere E, Pause BM, Pietrowsky R. Emotion and episodic memory in neuropsychiatric disorders. Behav Brain Res. 2010; 215:162–171. [PubMed: 20227444]

Everson-Rose SA, Mendes de Leon CF, Bienias JL, Wilson RS, Evans DA. Early life conditions and cognitive functioning in later life. Am J Epidemiol. 2003; 158:1083–1089. [PubMed: 14630604]

Goubran M, Hammond RR, de Ribaupierre S, Burneo JG, Mirsattari S, Steven DA, Parrent AG, Peters TM, Khan AR. Magnetic resonance imaging and histology correlation in the neocortex in temporal lobe epilepsy. Ann Neurol. 2015; 77:237–250. [PubMed: 25424188]

Hayes K, Buist R, Vincent TJ, Thiessen JD, Zhang Y, Zhang H, Wang J, Summers AR, Kong J, Li XM, Martin M. Comparison of manual and semi-automated segmentation methods to evaluate hippocampus volume in APP and PS1 transgenic mice obtained via in vivo magnetic resonance imaging. J Neurosci Methods. 2014; 221:103–111. [PubMed: 24091139]

Hodel AS, Hunt RH, Cowell RA, Van Den Heuvel SE, Gunnar MR, Thomas KM. Duration of early adversity and structural brain development in post-institutionalized adolescents. Neuroimage. 2015; 105:112–119. [PubMed: 25451478]

Holtmaat A, Svoboda K. Experience-dependent structural synaptic plasticity in the mammalian brain. Nat Rev Neurosci. 2009; 10:647–658. [PubMed: 19693029]

Ivy AS, Brunson KL, Sandman C, Baram TZ. Dysfunctional nurturing behavior in rat dams with limited access to nesting material: A clinically relevant model for early-life stress. Neuroscience. 2008; 154:1132–1142. [PubMed: 18501521]

Ivy AS, Rex CS, Chen Y, Dube C, Maras PM, Grigoriadis DE, Gall CM, Lynch G, Baram TZ. Hippocampal dysfunction and cognitive impairments provoked by chronic early-life stress involve excessive activation of CRH receptors. J Neurosci. 2010; 30:13005–13015. [PubMed: 20881118]

Kantarci K. Fractional anisotropy of the fornix and hippocampal atrophy in Alzheimer's disease. Front Aging Neurosci. 2014; 6:316. [PubMed: 25431558]

Kaplan GA, Turrell G, Lynch JW, Everson SA, Helkala EL, Salonen JT. Childhood socioeconomic position and cognitive function in adulthood. Int J Epidemiol. 2001; 30:256–263. [PubMed: 11369724]

Kehoe P, Bronzino JD. Neonatal stress alters LTP in freely moving male and female adult rats. Hippocampus. 1999; 9:651–658. [PubMed: 10641758]

Keller SS, Schoene-Bake JC, Gerdes JS, Weber B, Deppe M. Concomitant fractional anisotropy and volumetric abnormalities in temporal lobe epilepsy: Cross-sectional evidence for progressive neurologic injury. PLoS One. 2012; 7:e46791. [PubMed: 23071638]

Kerchner GA, Hess CP, Hammond-Rosenbluth KE, Xu D, Rabinovici GD, Kelley DA, Vigneron DB, Nelson SJ, Miller BL. Hippocampal CA1 apical neuropil atrophy in mild Alzheimer disease visualized with 7-T MRI. Neurology. 2010; 75:1381–1387. [PubMed: 20938031]

Kim CH, Koo BB, Chung CK, Lee JM, Kim JS, Lee SK. Thalamic changes in temporal lobe epilepsy with and without hippocampal sclerosis: A diffusion tensor imaging study. Epilepsy Res. 2010; 90:21–27. [PubMed: 20307957]

Kovacevic N, Henderson JT, Chan E, Lifshitz N, Bishop J, Evans AC, Henkelman RM, Chen XJ. A three-dimensional MRI atlas of the mouse brain with estimates of the average and variability. Cereb Cortex. 2005; 15:639–645. [PubMed: 15342433]

Krishnan V, Nestler EJ. The molecular neurobiology of depression. Nature. 2008; 455:894–902. [PubMed: 18923511]

Laitinen T, Sierra A, Bolkvadze T, Pitkanen A, Grohn O. Diffusion tensor imaging detects chronic microstructural changes in white and gray matter after traumatic brain injury in rat. Front Neurosci. 2015; 9:128. [PubMed: 25954146]

Langston RF, Wood ER. Associative recognition and the hippocampus: Differential effects of hippocampal lesions on object-place, object-context and object-place-context memory. Hippocampus. 2010; 20:1139–1153. [PubMed: 19847786]

Lyons DM, Yang C, Sawyer-Glover AM, Moseley ME, Schatzberg AF. Early life stress and inherited variation in monkey hippocampal volumes. Arch Gen Psychiatry. 2001; 58:1145–1151. [PubMed: 11735843]

Magarinos AM, McEwen BS. Stress-induced atrophy of apical dendrites of hippocampal CA3c neurons: comparison of stressors. Neuroscience. 1995; 69:83–88. [PubMed: 8637635]

Maras PM, Molet J, Chen Y, Rice C, Ji SG, Solodkin A, Baram TZ. Preferential loss of dorsal-hippocampus synapses underlies memory impairments provoked by short, multimodal stress. Mol Psychiatry. 2014; 19:811–822. [PubMed: 24589888]

McEwen BS. Early life influences on life-long patterns of behavior and health. Ment Retard Dev Disabil Res Rev. 2003; 9:149–154. [PubMed: 12953293]

McEwen BS. The ever-changing brain: Cellular and molecular mechanisms for the effects of stressful experiences. Dev Neurobiol. 2012; 72:878–890. [PubMed: 21898852]

McQuown SC, Barrett RM, Matheos DP, Post RJ, Rogge GA, Alenghat T, Mullican SE, Jones S, Rusche JR, Lazar MA, Wood MA. HDAC3 is a critical negative regulator of long-term memory formation. J Neurosci. 2011; 31:764–774. [PubMed: 21228185]

Millan MJ, Agid Y, Brune M, Bullmore ET, Carter CS, Clayton NS, Connor R, Davis S, Deakin B, DeRubeis RJ, Dubois B, Geyer MA, Goodwin GM, Gorwood P, Jay TM, Joels M, Mansuy IM, Meyer-Lindenberg A, Murphy D, Rolls E, Saletu B, Spedding M, Sweeney J, Whittington M, Young LJ. Cognitive dysfunction in psychiatric disorders: Characteristics, causes and the quest for improved therapy. Nat Rev Drug Discov. 2012; 11:141–168. [PubMed: 22293568]

Molet J, Maras PM, Avishai-Eliner S, Baram TZ. Naturalistic rodent models of chronic early-life stress. Dev Psychobiol. 2014; 56:1675–1688. [PubMed: 24910169]

Molet J, Heins K, Zhuo X, Mei YT, Regev L, Baram TZ, Stern H. Fragmentation and high entropy of neonatal experience predict adolescent emotional outcome. Transl Psychiatry. 2016; 6:e702. [PubMed: 26731439]

Nelson CA III, Zeanah CH, Fox NA, Marshall PJ, Smyke AT, Guthrie D. Cognitive recovery in socially deprived young children: The Bucharest early intervention project. Science. 2007; 318:1937–1940. [PubMed: 18096809]

Norris FC, Betts-Henderson J, Wells JA, Cleary JO, Siow BM, Walker-Samuel S, McCue K, Salomoni P, Scambler PJ, Lythgoe MF. Enhanced tissue differentiation in the developing mouse brain using magnetic resonance micro-histology. Magn Reson Med. 2013; 70:1380–1388. [PubMed: 23213043]

O'Doherty DC, Chitty KM, Saddiqui S, Bennett MR, Lagopoulos J. A systematic review and meta-analysis of magnetic resonance imaging measurement of structural volumes in posttraumatic stress disorder. Psychiatry Res. 2015; 232:1–33. [PubMed: 25735885]

Papp EA, Leergaard TB, Calabrese E, Johnson GA, Bjaalie JG. Waxholm Space atlas of the Sprague Dawley rat brain. NeuroImage. 2014; 97:374–386. [PubMed: 24726336]

Paus, T. Individual bases of adolescent development. In: Lerner, RM., Steinberg, L., editors. Handbook of Adolescent Psychology. 3. Hoboken, New Jersey: Wiley; 2009. p. 95-115.

Pawlak R, Rao BS, Melchor JP, Chattarji S, McEwen B, Strickland S. Tissue plasminogen activator and plasminogen mediate stress-induced decline of neuronal and cognitive functions in the mouse hippocampus. Proc Natl Acad Sci USA. 2005; 102:18201–18206. [PubMed: 16330749]

Pych JC, Vankatasubramanian PN, Faulkner J, Wyrwicz A. Decreased hippocampal fractional anisotropy in Tg2576 Alzheimer's disease–model mice may reflect a reduction in dendrites. Alzheimer's Dementia. 2008; 4:T71–T72.

Qiu A, Mori S, Miller MI. Diffusion tensor imaging for understanding brain development in early life. Annu Rev Psychol. 2015; 66:853–876. [PubMed: 25559117]

Radley JJ, Rocher AB, Rodriguez A, Ehlenberger DB, Dammann M, McEwen BS, Morrison JH, Wearne SL, Hof PR. Repeated stress alters dendritic spine morphology in the rat medial prefrontal cortex. J Comp Neurol. 2008; 507:1141–1150. [PubMed: 18157834]

Regev L, Baram TZ. Corticotropin releasing factor in neuroplasticity. Front Neuroendocrinol. 2014; 35:171–179. [PubMed: 24145148]

Rice CJ, Sandman CA, Lenjavi MR, Baram TZ. A novel mouse model for acute and long-lasting consequences of early life stress. Endocrinology. 2008; 149:4892–4900. [PubMed: 18566122]

Schoemaker D, Buss C, Head K, Sandman CA, Davis EP, Chakravarty MM, Gauthier S, Pruessner JC. Hippocampus and amygdala volumes from magnetic resonance images in children: Assessing accuracy of FreeSurfer and FSL against manual segmentation. NeuroImage. 2016; 129:1–14. [PubMed: 26824403]

Segal M, Richter-Levin G, Maggio N. Stress-induced dynamic routing of hippocampal connectivity: A hypothesis. Hippocampus. 2010; 20:1332–1338. [PubMed: 20082290]

Shenton ME, Hamoda HM, Schneiderman JS, Bouix S, Pasternak O, Rathi Y, Vu MA, Purohit MP, Helmer K, Koerte I, Lin AP, Westin CF, Kikinis R, Kubicki M, Stern RA, Zafonte R. A review of magnetic resonance imaging and diffusion tensor imaging findings in mild traumatic brain injury. Brain Imaging Behav. 2012; 6:137–192. [PubMed: 22438191]

Sholl DA. Dendritic organization in the neurons of the visual and motor cortices of the cat. J Anat. 1953; 87:387–406. [PubMed: 13117757]

Sierra A, Laitinen T, Grohn O, Pitkanen A. Diffusion tensor imaging of hippocampal network plasticity. Brain Struct Funct. 2015; 220:781–801. [PubMed: 24363120]

Squire LR, Wixted JT, Clark RE. Recognition memory and the medial temporal lobe: A new perspective. Nat Rev Neurosci. 2007; 8:872–883. [PubMed: 17948032]

Teicher MH, Anderson CM, Polcari A. Childhood maltreatment is associated with reduced volume in the hippocampal subfields CA3, dentate gyrus, and subiculum. Proc Natl Acad Sci USA. 2012; 109:E563–E572. [PubMed: 22331913]

Trivedi R, Gupta RK, Husain N, Rathore RK, Saksena S, Srivastava S, Malik GK, Das V, Pradhan M, Sarma MK, Pandey CM, Narayana PA. Region-specific maturation of cerebral cortex in human fetal brain: Diffusion tensor imaging and histology. Neuroradiology. 2009; 51:567–576. [PubMed: 19421746]

Ulrich-Lai YM, Herman JP. Neural regulation of endocrine and autonomic stress responses. Nat Rev Neurosci. 2009; 10:397–409. [PubMed: 19469025]

van Haren NE, Picchioni MM, McDonald C, Marshall N, Davis N, Ribchester T, Hulshoff Pol HE, Sharma T, Sham P, Kahn RS, Murray R. A controlled study of brain structure in monozygotic

twins concordant and discordant for schizophrenia. Biol Psychiatry. 2004; 56:454–461. [PubMed: 15364044]

Vogel-Ciernia A, Wood MA. Examining object location and object recognition memory in mice. Curr Protoc Neurosci. 2014; 69:8.31.1–8.31.17. [PubMed: 25297693]

Wang XD, Rammes G, Kraev I, Wolf M, Liebl C, Scharf SH, Rice CJ, Wurst W, Holsboer F, Deussing JM, Baram TZ, Stewart MG, Muller MB, Schmidt MV. Forebrain CRF(1) modulates early-life stress-programmed cognitive deficits. J Neurosci. 2011; 31:13625–13634. [PubMed: 21940453]

Wang XD, Labermaier C, Holsboer F, Wurst W, Deussing JM, Muller MB, Schmidt MV. Early-life stress-induced anxiety-related behavior in adult mice partially requires forebrain corticotropin-releasing hormone receptor 1. Eur J Neurosci. 2012; 36:2360–2367. [PubMed: 22672268]

Wilson RS, Scherr PA, Bienias JL, Mendes de Leon CF, Everson-Rose SA, Bennett DA, Evans DA. Socioeconomic characteristics of the community in childhood and cognition in old age. Exp Aging Res. 2005; 31:393–407. [PubMed: 16147459]

Woon FL, Hedges DW. Hippocampal and amygdala volumes in children and adults with childhood maltreatment-related post-traumatic stress disorder: A meta-analysis. Hippocampus. 2008; 18:729–736. [PubMed: 18446827]

Yassa MA, Muftuler LT, Stark CE. Ultrahigh-resolution microstructural diffusion tensor imaging reveals perforant path degradation in aged humans in vivo. Proc Natl Acad Sci USA. 2010; 107:12687–12691. [PubMed: 20616040]

Zalsman G, Gutman A, Shbiro L, Rosenan R, Mann JJ, Weller A. Genetic vulnerability, timing of short-term stress and mood regulation: A rodent diffusion tensor imaging study. Eur Neuropsychopharmacol J Eur Coll Neuropsychopharmacol. 2015; 25:2075–2085.

Zhang J, van Zijl PC, Mori S. Three-dimensional diffusion tensor magnetic resonance microimaging of adult mouse brain and hippocampus. NeuroImage. 2002; 15:892–901. [PubMed: 11906229]

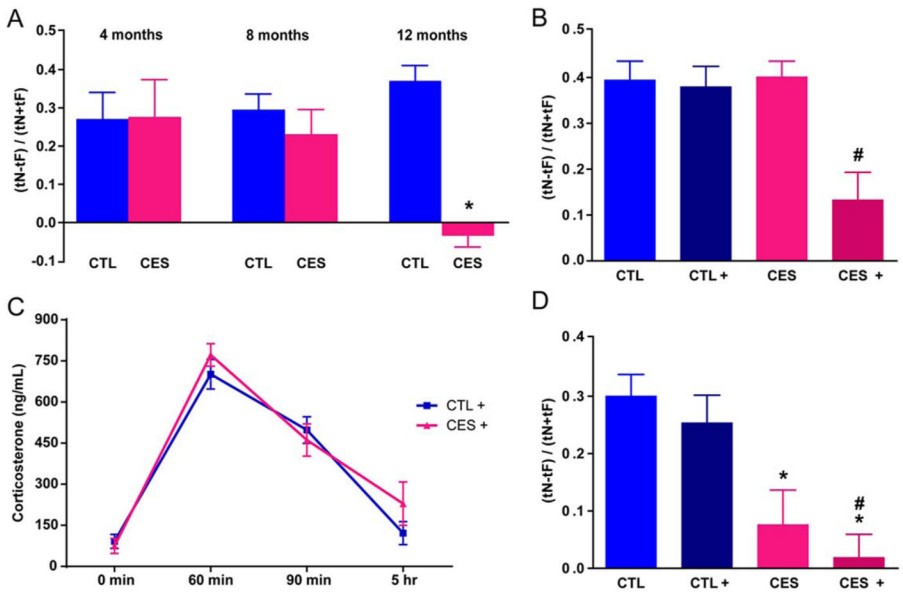

FIGURE 1.

Chronic early-life stress (CES) provokes incipient and overt memory impairments. A: Using object recognition tests, both control (CTL) and (CES) rats (n =6/group) spent more time exploring the novel (N) compared to familiar (F) object at ages 4 and 8 months. However, by 12 months, CES rats failed to distinguish the objects. B: Already at 2 months, stress challenge uncovered incipient impairments of object memory in CES rats. 24 h after a short (5 h) stress, CES+ rats, but not CTL+ rats failed to spend more time exploring the novel vs. the familiar object (n =8–11/group). C: The impaired memory did not result from anxiety (see text) or altered stress-responses in CES rats: the time-course of plasma corticosterone was comparable between groups. (n =12/group/time-point). Statistical significance is denoted by $^{*}P < 0.05$ compared to CTL, $^{\#}P < 0.05$ compared to CTL, CTL+, and CES. D: Hippocampus-dependent spatial memory (object location/placement, OL) was impaired in CES rats already at age 2 months. These rats failed to spend more time exploring the novel compared to familiar locations, indicated by the discrimination index (DI) values. These deficits were apparent with (CES+) or without (CES) exposure to a short stress 24 h earlier. Error bars indicate SEM. [Color figure can be viewed at wileyonlinelibrary.com]

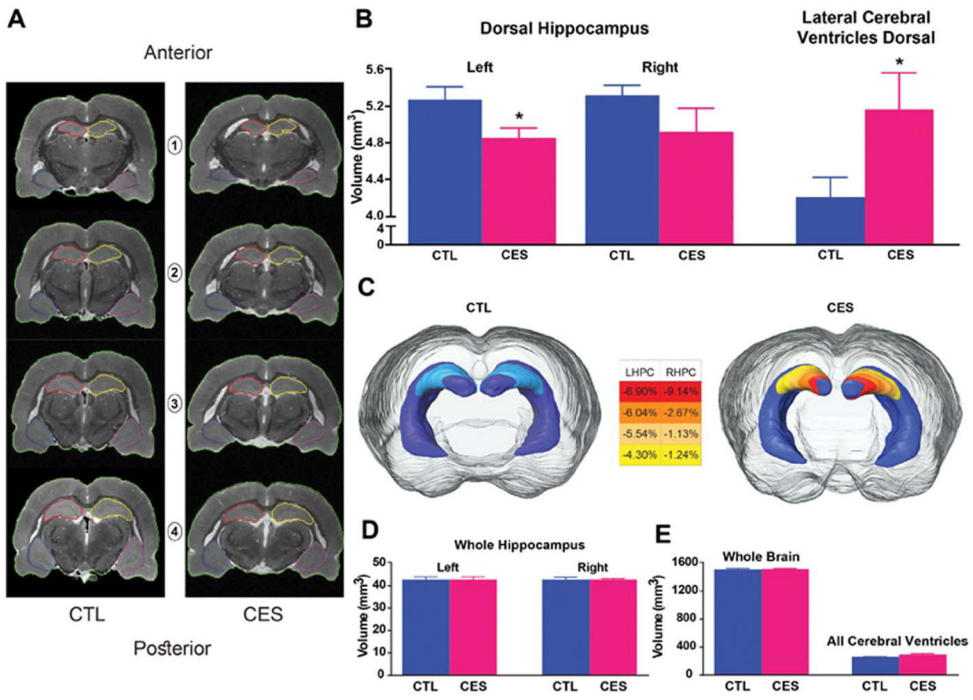

FIGURE 2.

CES reduces the volume of dorsal hippocampus subregions involved in memory. Volumetric analyses of brain and hippocampus were performed on 3D-RARE coronal MRI sections (78 μm; see Methods). A: Representative regions of interest illustrate boundaries of left hippocampus (red), right hippocampus (yellow) and brain (green). B: Left mid-dorsal hippocampal volumes were reduced (*left*) with corresponding increase of volumes of lateral cerebral ventricles in the same mid-dorsal sections (*right*) in CES rats (see Methods for precise definitions and boundaries). C: three-dimensional rendering of hippocampus illustrates decreased mid-dorsal hippocampal volume in CES rats. The color-coded scale indicates the average percent of volume reduction of each hemisphere in the CES vs. CTL rats. D: The sub-regional volume reduction is insufficient to alter total volumes of the whole left or right hippocampi or E: of brain and cerebral ventricles. Statistical significance is denoted by $*P < 0.05$ vs. CTL. Error bars indicate SEM. [Color figure can be viewed at wileyonlinelibrary.com]

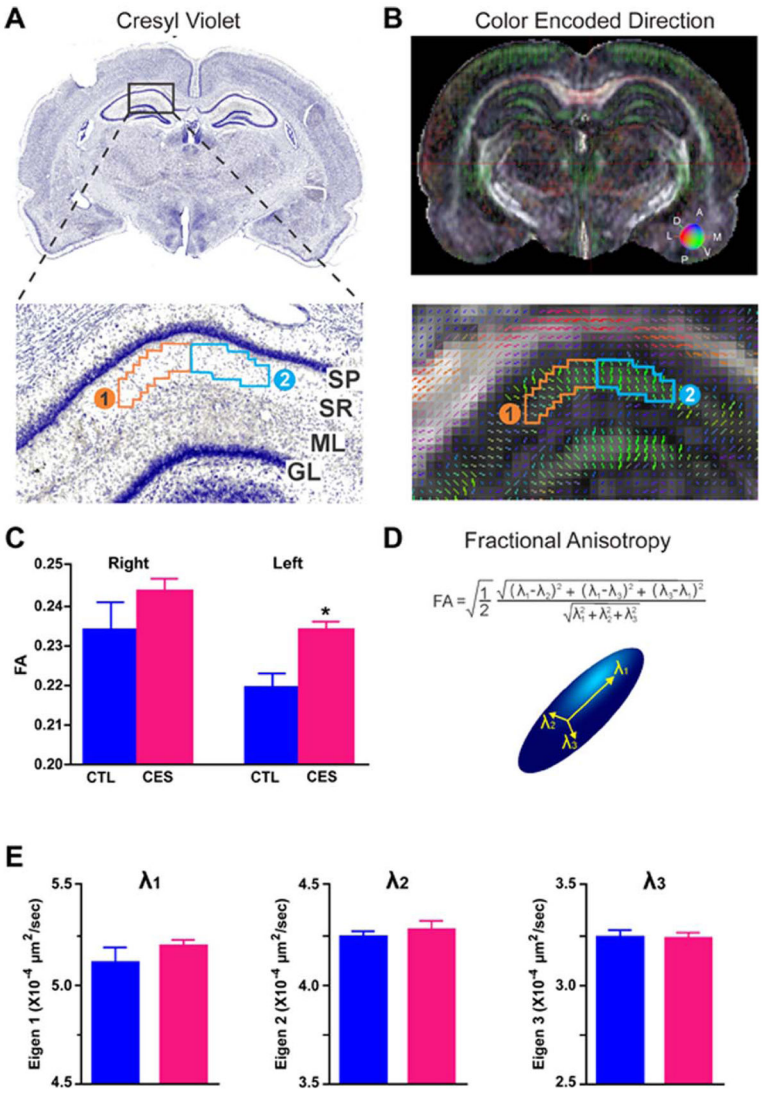

FIGURE 3.

Diffusion tensor imaging (DTI) identifies microstructural alterations provoked by CES. In images obtained using high-resolution, 30-direction DTI, two regions of interest (ROI) within CA1 dendritic layers were delineated and analyzed. A: Stratum radiatum (SR) delineated on fractional anisotropy (FA) maps B: via anatomical landmarks (see Methods). Because directional vectors within CA1-SR vary along the mediolateral axis, the region was divided into two ROIs. Group-specific differences were confined to ROI-1. C: FA (water mobility asymmetry) was significantly ($P < 0.01$) increased in 7- to 8-week old CES rats compared to controls (CTL). D: FA represents the anisotropy from three eigenvalues (λ), illustrated by the diffusion ellipsoid. Therefore, E: the contribution of each eigenvalue (λ1, λ2, λ3) to the increased FA is shown. Increased FA is a result of trends for increased λ1 and λ2 values. Statistical significance is denoted by $*P < 0.05$ vs. CTL. Error bars indicate SEM. SP, stratum pyramidale; ML, molecular layer; GL, granule cell layer. [Color figure can be viewed at wileyonlinelibrary.com]

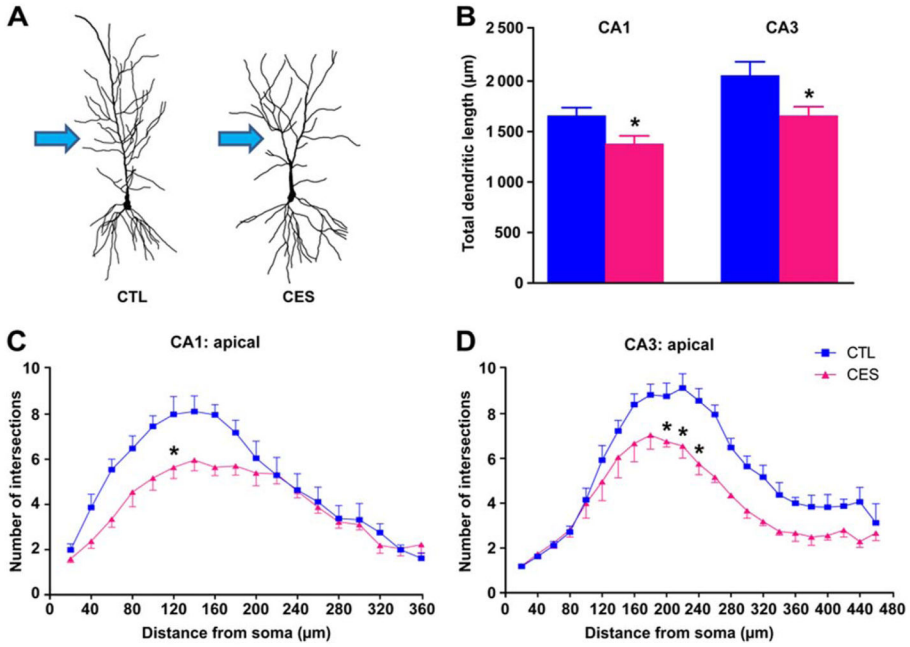

FIGURE 4.

Dendritic tree abnormalities in CES hippocampus underlie the volume loss and abnormal microstructure identified by MRI and DTI. A: Representative neurons from each group illustrate reduced dendritic arborization in CES CA1 neurons. B: Total apical dendritic lengths in hippocampal areas CA1 and CA3 were significantly reduced in CES rats (n =3–4/group). C: Complexity of dendritic arbors was quantified using Sholl analyses, counting numbers of dendritic intersections in apical dendritic hippocampal CA1 and D: CA3 regions. Dendritic complexity was diminished in CES rats vs. CTL (n =6–10 neurons/rat). Statistical significance is denoted by *P < 0.05 vs. CTL. Error bars indicate SEM. [Color figure can be viewed at wileyonlinelibrary.com]

TABLE 1

Parameters of the Object Recognition Test (OR) in Training and Testing Phases Following Chronic Early-Life Stress (CES)

	4 Months			8 Months			12 Months			
	CTL	**CES**	***P* value**	**CTL**	**CES**	***P* value**	**CTL**	**CES**	***P* value**	**ANOVA value**
Total exploration time of training phase	76.44 ±8.73	75.75 ±6.63	*n.s*	52.57 ±5.14	41.28 ±3.77	*n.s*	38.33 ±4.16	33.34 ±2.62	*n.s*	Age: $F_{(2.20)}$ = 30.34; P <0.0001; CES: $F_{(1.10)}$ = 1.355; P =0.272; Interaction: $F_{(2.20)}$ = 0.4986; P =0.615
Ratio of training phase	1.107 ±0.08	0.870 ±0.04	*n.s*	0.972 ±0.07	0.915 ±0.06	*n.s*	1.038 ±0.10	0.942 ±0.88	*n.s*	Age: $F_{(2.20)}$ = 0.2155; P =0.808; CES: $F_{(1.10)}$ = 3.058; P =0.111; Interaction: $F_{(2.20)}$ = 0.9487; P =0.404
Discrimination index of training phase	0.044 ±0.04	−0.072 ±0.02	*n.s*	−0.021 ±0.04	−0.048 ±0.03	*n.s*	0.008 ±0.05	−0.041 ±0.05	*n.s*	
Total exploration time of testing phase	57.77 ±6.27	48.40 ±5.30	*n.s*	34.7 ±3.45	33.06 ±3.62	*n.s*	30.95 ±4.02	28.67 ±3.10	*n.s*	Age: $F_{(2.20)}$ = 15.29; P <0.0001; CES: $F_{(1.10)}$ = 1.583; P =0.237 Interaction: $F_{(2.20)}$ = 0.4552; P =0.641
Ratio of testing phase	1.872 ±0.28	2.063 ±0.48	*n.s*	1.888 ±0.18	1.688 ±0.22	*n.s*	2.243 ±0.20	0.94 ±0.06	*s*	Age: $F_{(2.20)}$ = 1.867; P =0.181 ; CES: $F_{(1.10)}$ = 7.964; P =0.018 ; Interaction: $F_{(2.20)}$ = 6.800; P =0.0056
Discrimination index of testing phase	0.270 ±0.07	0.275 ±0.10	*n.s*	0.294 ±0.04	0.230 ±0.07	*n.s*	0.371 ±0.04	−0.034 ±0.03	*s*	

Durations of exploration (in sec) during the OR task were similar among groups. During the training phase, total exploration of the two identical objects, as well as the discrimination ratio or the discrimination index (DI) between these objects were comparable in CTL and CES rats. During the testing phase, the total exploration time did not differ between the both groups. At 4 and 8 months, both CTL and CES rats spent more time exploring the novel object, whereas at 12 months CES rats failed to distinguish the novel from the familiar object. The object memory function of the CES rats declined with the age. Data are presented as mean (± SEM) and were analyzed using two-way repeated measure (RM)-ANOVA, followed by Bonferroni's post hoc multiple comparisons test. Abbreviations: CTL, control; CES, chronic early-life stressed; DI, discrimination index; n.s, non-significant; s, significant. Significance levels were set at 0.05.

TABLE 2

Parameters of the Object Recognition Test (OR) During Training and Testing Phases Following Chronic Early-life Stress (CES) and an Acute Challenge

	No challenge		Challenge			*P* value					
	CTL	**CES**	**CTL+**	**CES+**	**ANOVA value**	**CTL *vs.* CES**	**CTL *vs.* CTL+**	**CTL *vs.* CES+**	**CTL+ *vs.* CES**	**CTL+ *vs.* CES+**	**CES *vs.* CES+**
Total exploration time of training phase	69.92 ±4.86	68.45 ±7.57	65.03 ±6.48	74.62 ±6.93	CES: $F_{(1.34)}$ = 0.359; P =0.553; Challenge: $F_{(1.34)}$ = 0.009; P=0.925; Interaction: $F_{(1.34)}$ = 0.668; P=0.420	n.s	n.s	n.s	n.s	n.s	n.s
Ratio of training phase	0.953 ±0.06	0.966 ±0.05	1.008 ±0.07	1.076 ±0.05	CES: $F_{(1.34)}$ = 0.432; P =0.516 Challenge: $F_{(1.34)}$ = 1.768; P=0.193; nteraction: $F_{(1.34)}$ = 0.191; P=0.665	n.s	n.s	n.s	n.s	n.s	n.s
Discrimination index of training phase	−0.031 ±0.03	−0.023 ±0.03	−0.008 ±0.03	0.030 ±0.02	CES: $F_{(1.34)}$ = 0.591; P =0.447; Challenge: $F_{(1.34)}$ = 1.648; P=0.208; Interaction: $F_{(1.34)}$ = 0.191; P=0.665	n.s	n.s	n.s	n.s	n.s	n.s
Total exploration time of testing phase	51.81 ±4.58	51.54 ±4.89	41.50 ±4.26	49.40 ±3.76	CES: $F_{(1.34)}$ = 0.756; P =0.391; Challenge: $F_{(1.34)}$ = 2.013; P=0.165; Interaction: $F_{(1.34)}$ = 0.869; P=0.358	n.s	n.s	n.s	n.s	n.s	n.s
Ratio of testing phase	2.419 ±0.25	2.416 ±0.19	2.407 ±0.26	1.436 ±0.20	CES: $F_{(1.34)}$ = 4.364; P =0.044; Challenge: $F_{(1.34)}$ = 4.526; P=0.041; Interaction:	ns	n.s	s	n.s	s	s

	No challenge		Challenge			*P* value					
	CTL	**CES**	**CTL+**	**CES+**	**ANOVA value**	**CTL *vs*. CES**	**CTL *vs*. CTL+**	**CTL *vs*. CES+**	**CTL+ *vs*. CES**	**CTL+ *vs*. CES+**	**CES *vs*. CES+**
					$F_{(1.34)} = 4.319$; $P = 0.045$						
Discrimination index of testing phase	0.394 ±0.04	0.401 ±0.03	0.380 ±0.04	0.133 ±0.06	CES: $F_{(1.34)} = 5.830$; $P = 0.021$; Challenge: $F_{(1.34)} = 8.123$; $P = 0.007$; Interaction: $F_{(1.34)} = 6.537$; $P = 0.015$	ns	n.s	s	n.s	s	s

During the training phase, the total exploration (in sec), the discrimination ratio and the discrimination index (DI) were similar among groups. During the testing phase, the total exploration time did not differ between the four groups. Memory performance task was not altered by the short (5-h) multi-modal stress (challenge) in control group or by the early-life adversity alone during the late adolescence. However, after this new challenge, CES rats failed to distinguish the novel object from the familiar object. Data are presented as mean (± SEM) and were analyzed using two-way ANOVA, followed by Bonferroni's post hoc multiple comparisons test. Abbreviations: CTL, control; CTL+, challenged CTL; CES, chronic early-life stressed; CES+, challenged CES; DI, discrimination index; n.s, non-significant; s, significant. Significance levels were set at 0.05.

TABLE 3

Parameters of the Hippocampus-dependent Object Location Test (OL) During Training and Testing Phases Following Chronic Early-life Stress (CES) and an Acute Challenge

	No challenge		Challenge			*P* value					
	CTL	**CES**	**CTL+**	**CES+**	**ANOVAvalue**	**CTL *vs.* CES**	**CTL *vs.* CTL+**	**CTL *vs.* CES+**	**CTL+ *vs.* CES**	**CTL+ *vs.* CES+**	**CES *vs.* CES+**
Total exploration time of training phase	97.12 ±10.39	89.77 ±11.32	91.00 ±10.65	102.2 ±10.35	CES: $F_{(1.73)}$ = 0.032; *P* =0.859; Challenge: $F_{(1.73)}$ = 0.086; *P* =0.771; Interaction: $F_{(1.73)}$ = 0.744; *P* =0.392	n.s	n.s	n.s	n.s	n.s	n.s
Ratio of training phase	1.150 ±0.70	1.110 ±0.08	0.967 ±0.06	1.072 ±0.09	CES: $F_{(1.73)}$ = 0.205; *P* =0.652; Challenge: $F_{(1.73)}$ = 2.314; *P* =0.133; Interaction: $F_{(1.73)}$ = 0.985; *P* =0.324	n.s	n.s	n.s	n.s	n.s	n.s
Discrimination index of training phase	−0.052 ±0.03	−0.034 ±0.03	−0.035 ±0.03	0.007 ±0.04	CES: $F_{(1.73)}$ = 0.134; *P* =0.715; Challenge: $F_{(1.73)}$ = 3.076; *P* =0.084; Interaction: $F_{(1.73)}$ = 0.845; *P* =0.361	n.s	n.s	n.s	n.s	n.s	n.s
Total exploration time of testing phase	60.16 ±6.82	61.31 ±6.01	54.22 ±6.97	68.24 ±5.96	CES: $F_{(1.73)}$ = 1.338; *P* =0.251; Challenge: $F_{(1.73)}$ = 0.006; *P* =0.940; Interaction: $F_{(1.73)}$ =	n.s	n.s	n.s	n.s	n.s	n.s

	No challenge		Challenge			*P* value					
	CTL	**CES**	**CTL+**	**CES+**	**ANOVAvalue**	**CTL *vs*. CES**	**CTL *vs*. CTL+**	**CTL *vs*. CES+**	**CTL+ *vs*. CES**	**CTL+ *vs*. CES+**	**CES *vs*. CES+**
					0.964; P =0.329						
Ratio of testing phase	2.10 ±0.25	1.36 ±0.18	1.90 ±0.19	1.10 ±0.09	CES: $F_{(1.73)}$ = 15.490; P <0.001; Challenge: $F_{(1.73)}$ = 1.411; P =0.239; Interaction: $F_{(1.73)}$ = 0.027; P =0.869	s	ns	s	ns	s	ns
Discrimination index of testing phase	0.300 ±0.04	0.076 ±0.06	0.254 ±0.05	0.189 ±0.04	CES: $F_{(1.73)}$ = 23.23; P <0.001; Challenge: $F_{(1.73)}$ = 1.191; P =0.279; Interaction: $F_{(1.73)}$ = 0.013; P =0.911	s	ns	s	ns	s	ns

During the training phase of the hippocampus-dependent object location (OL), all parameters of the test: the total exploration, the discrimination ratio and discrimination index (DI) were similar among groups. During the testing phase of the OL task, the discrimination ratio or the DI demonstrated that CES rats exposed or not to the short (5-h) multi-modal stress (challenge) failed to distinguish the familiar location from the novel one. Data are presented as mean (± SEM) and were analyzed using two-way ANOVA, followed by Bonferroni's post hoc multiple comparisons test. Abbreviations: CTL, control; CTL+, challenged CTL; CES, chronic early-life stressed; CES+, challenged CES; DI, discrimination index; n.s, non-significant; s, significant. Significance levels were set at 0.05.

TABLE 4

DTI Parameters Extracted from the CA1 Apical Dendritic Region of the Hippocampus

Parameter	CTL right	CES right	CTL left	CES left
FA	0.234 ±0.007	0.244 ±0.003	0.220 ±0.003	0.234 ±0.002
λ1*	5.103 ±0.059	5.107 ±0.044	5.115 ±0.077	5.199 ±0.030
λ2*	4.183 ±0.039	4.129 ±0.022	4.244 ±0.029	4.282 ±0.047
λ3*	3.102 ±0.030	3.146 ±0.029	3.243 ±0.038	3.238 ±0.030
RD*	3.619 ±0.023	3.629 ±0.027	3.754 ±0.021	3.759 ±0.033

Fractional anisotropy (FA) increased in CES compared to CTL rats. In the left hippocampus of CES rats, the increased FA was associated with trends in changes, along the plane of the main apical dendritic stem (λ1), as well as water mobility within the plane of the commissural-associational and Schaeffer collateral branching (λ2). However, there was any discernible difference in the anterior-posterior direction (λ3), as well as radial diffusivity (RD). Together, these findings suggest that FA is the best predictor of altered diffusion in the apical dendritic CA1 region of the hippocampus after CES, wherein λ1 and 2 might be the largest contributors. Data are presented as mean (± SEM) and were analyzed using one-way ANOVA, followed by Tukey's post hoc multiple comparisons test. Abbreviations: CTL, control; CES, chronic early-life stressed; FA, fractional anisotropy; RD, radial diffusivity. Statistical significance is denoted by * $X10^{-4}$ μm^2 s^{-1}.